

Supporting Information for

# Electrochemical Tuning of MoS<sub>2</sub> Nanoparticles on Three-Dimensional Substrate for Efficient Hydrogen Evolution

*Haotian Wang*<sup>1,†</sup>, *Zhiyi Lu*<sup>2,†</sup>, *Desheng Kong*<sup>2</sup>, *Jie Sun*<sup>2</sup>, *Thomas M. Hymel*<sup>2</sup>, and *Yi Cui*<sup>2,3,\*</sup>

<sup>1</sup>Department of Applied Physics, Stanford University, Stanford, CA 94305, USA

<sup>2</sup>Department of Materials Science and Engineering, Stanford University, Stanford, CA 94305, USA

<sup>3</sup>Stanford Institute for Materials and Energy Sciences, SLAC National Accelerator Laboratory, 2575 Sand Hill Road, Menlo Park, California 94025, USA

†These authors contributed equally.

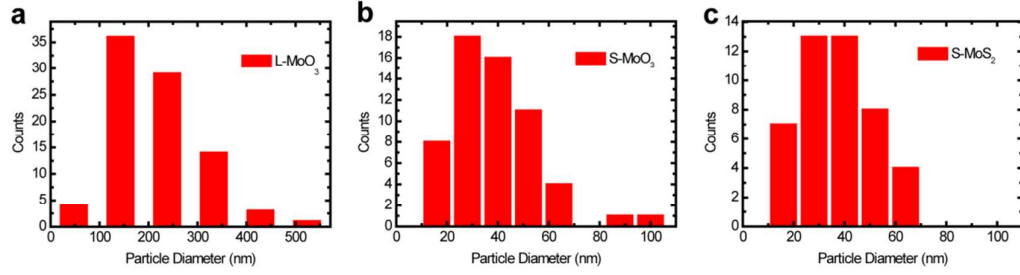


**Figure S1.** Statistical analysis of the particle size distributions of L-MoO<sub>3</sub>, S-MoO<sub>3</sub>, and S-MoS<sub>2</sub> respectively. The size of L-MoO<sub>3</sub> NP is ~ 200 nm, much larger than those of S-MoO<sub>3</sub> and S-MoS<sub>2</sub> which are ~ 30 nm.

*L-MoS<sub>2</sub> and S-MoS<sub>2</sub> NP surface area estimation:*

We treat the NP as a perfect sphere to simplify the calculation process. The diameters of L-MoS<sub>2</sub> and S-MoS<sub>2</sub> are 200 and 30 nm respectively. The mass loading  $m_L$  and  $m_S$  of the catalysts are the same. We set that the numbers of L-MoS<sub>2</sub> and S-MoS<sub>2</sub> per area on CFP are  $N_L$  and  $N_S$  respectively, and we can easily get the equation shown below:

$$m_L = N_L \frac{4}{3} \pi (100 \text{ nm})^3 \rho,$$

$$m_S = N_S \frac{4}{3} \pi (15 \text{ nm})^3 \rho,$$

$$m_L = m_S \rightarrow N_S = \left(\frac{100}{15}\right)^3 N_L,$$

where  $\rho$  represents the density of MoS<sub>2</sub>. Then we can get the surface area ratio of S-MoS<sub>2</sub> to L-MoS<sub>2</sub> as:

$$\frac{S_S}{S_L} = \frac{N_S 4\pi (15 \text{ nm})^2}{N_L 4\pi (100 \text{ nm})^2} = \frac{100}{15} = 6.7.$$

This rough estimation agrees well with the electrochemical capacitance measurement which gives out a result of 3.6.

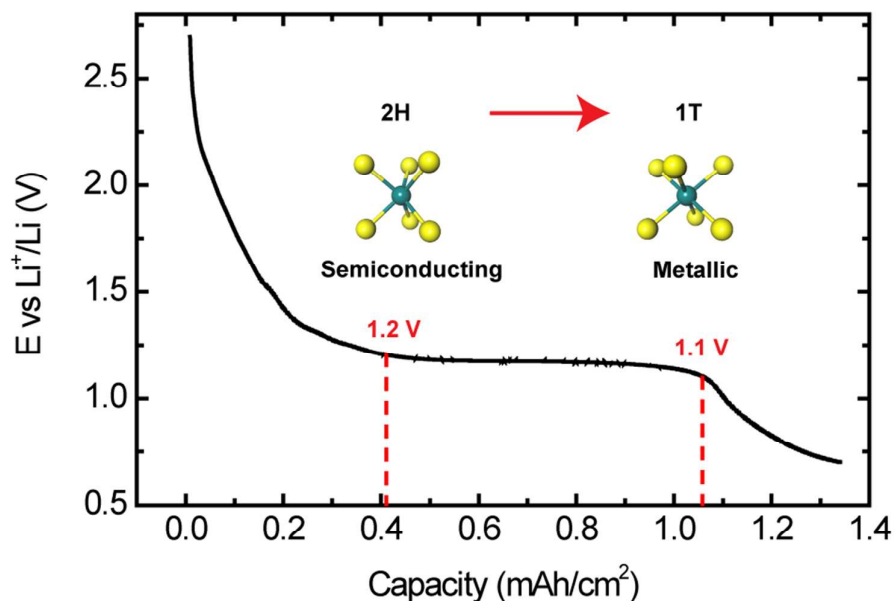


**Figure S2.** Galvanostatic discharge curve of Li electrochemical intercalation into MoS<sub>2</sub> NPs. The well-defined plateau from 1.2 to 1.1 V vs. Li<sup>+</sup>/Li represents the 2H to 1T phase transition. The atomic structure is changed from trigonal prismatic to octahedral, along with the electronic semiconducting to metallic transition. The capacity, which is 0.65  $\text{mAh}/\text{cm}^2$  as shown in the figure, of the plateau offers us the mass loading of MoS<sub>2</sub>. From Ref. 10 we know that during the phase transition process the Li composition changes by about  $\Delta x \approx 1$ , therefore we can calculate the mass loading of MoS<sub>2</sub> to be 3.88  $\text{mg}/\text{cm}^2$ , which agrees well with the measurement by microbalance.

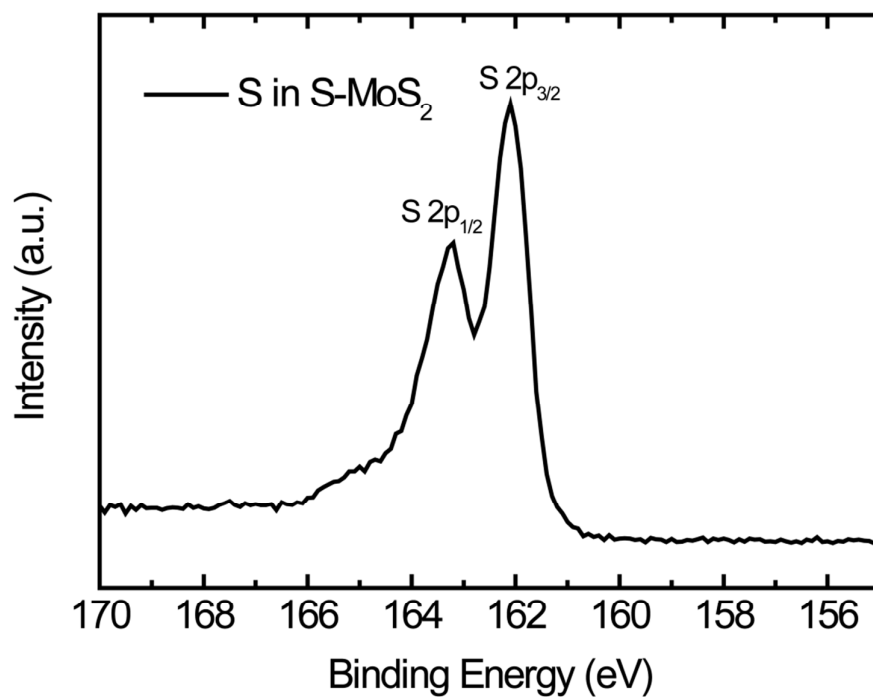


**Figure S3.** XPS spectra of S in S-MoS<sub>2</sub> catalyst. The peak positions of S 2p<sub>1/2</sub> and 2p<sub>3/2</sub> are 163.2 and 162.1 eV respectively.

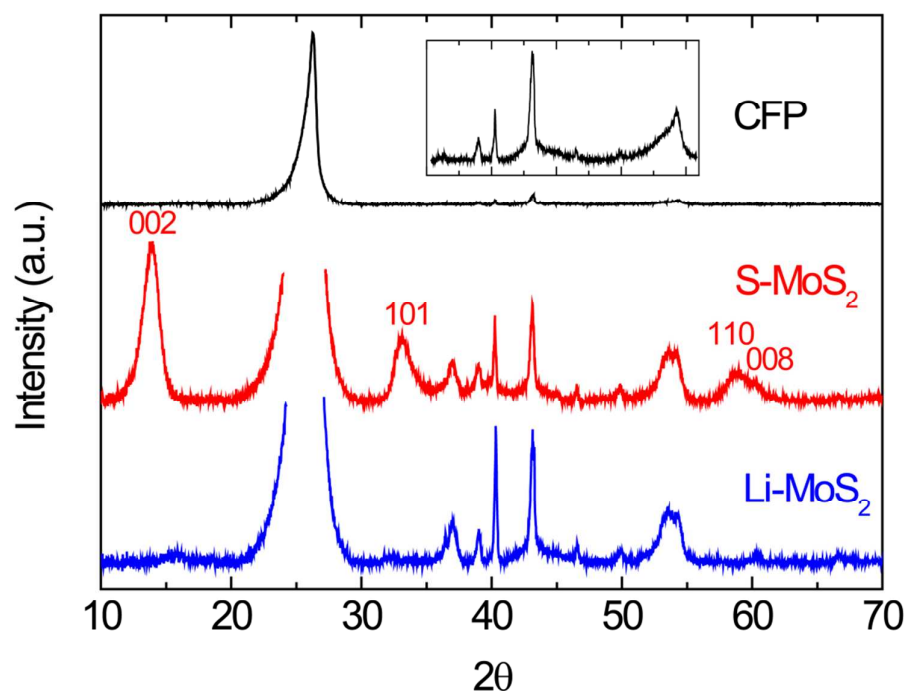


**Figure S4.** X-ray diffraction spectra of the substrate background, S-MoS<sub>2</sub>, and Li-MoS<sub>2</sub>. CFP has a very strong peak which is truncated for amplification of other peaks. The additional small peaks of CFP are zoomed in as shown by the inset. Distinguished peaks of MoS<sub>2</sub> are marked in the spectrum of S-MoS<sub>2</sub>. However, after the lithiation and exfoliation processes those peaks disappear in Li-MoS<sub>2</sub> spectrum.

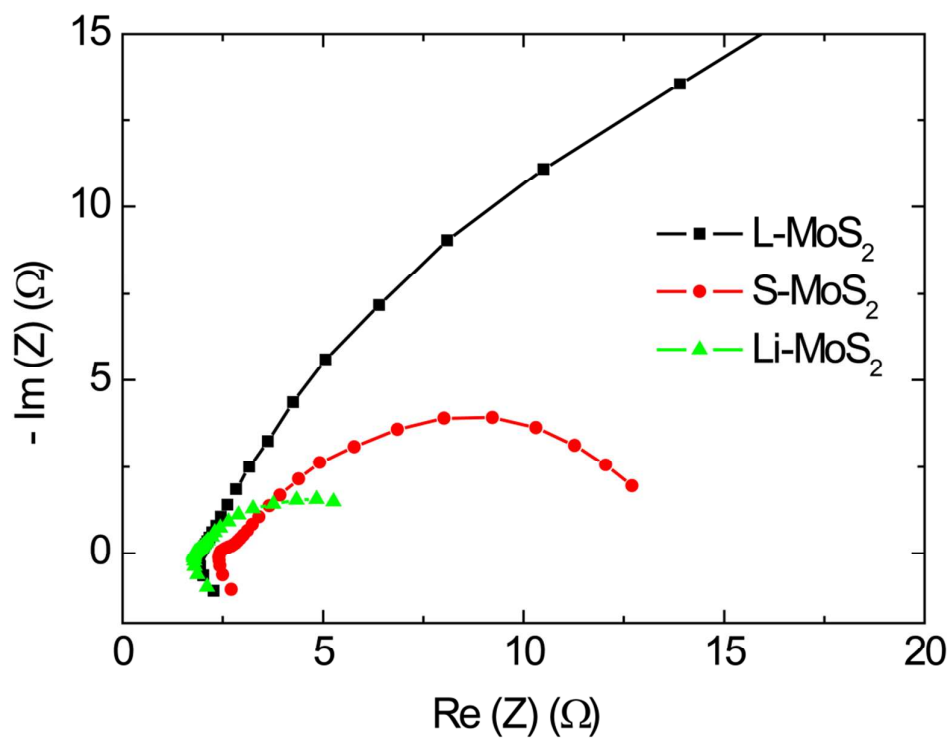


**Figure S5.** Nyquist plots of impedance spectroscopy analysis of the electrochemical cells setup, where L-MoS<sub>2</sub>, S-MoS<sub>2</sub>, and Li-MoS<sub>2</sub> were used as working electrodes. The series resistances are 1.92 Ω for L-MoS<sub>2</sub>, 2.43 Ω for S-MoS<sub>2</sub>, and 1.80 Ω for Li-MoS<sub>2</sub> respectively. The series resistance primarily comes from wiring and the electrolyte, while the resistance of MoS<sub>2</sub> NPs is negligible.

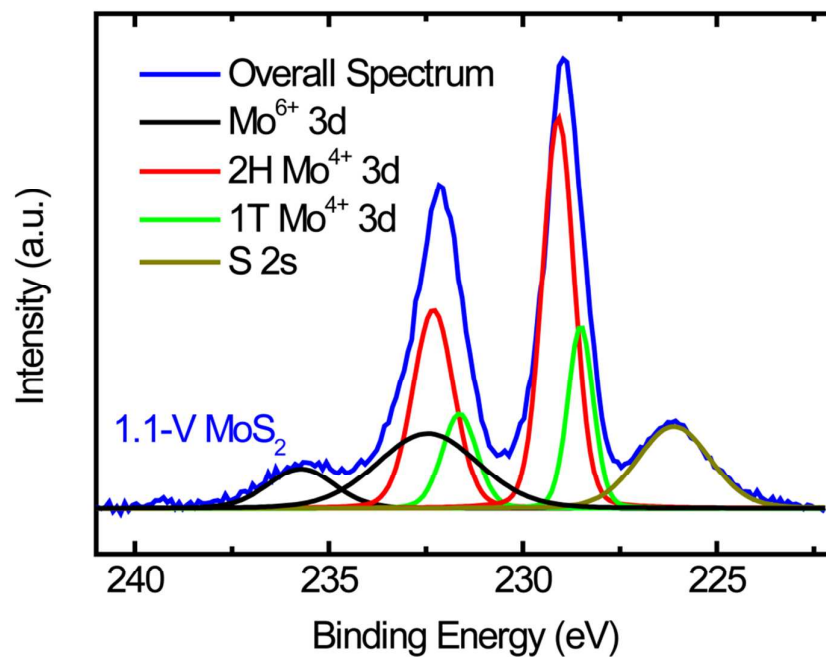


**Figure S6.** XPS spectrum of the 1.1-V MoS<sub>2</sub> sample. The broad Mo regions in 1.1-V MoS<sub>2</sub> spectrum is deconvoluted into red and green peaks, corresponding to 2H MoS<sub>2</sub> and 1T MoS<sub>2</sub> respectively. The ratio of MoS<sub>2</sub> 2H to 1T phase is estimated to be 2.67 by the Mo 3d<sub>5/2</sub> peak intensities.

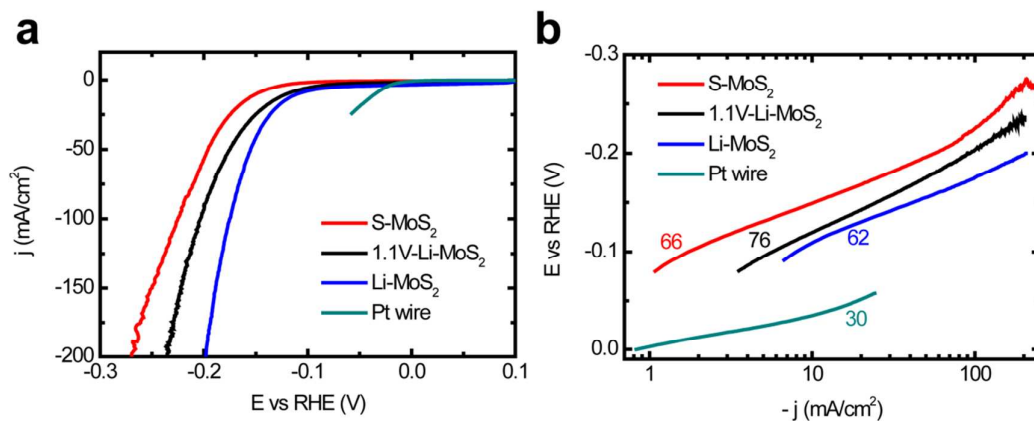


**Figure S7.** Comparison of HER performances of S-MoS<sub>2</sub>, 1.1-V MoS<sub>2</sub>, and Li-MoS<sub>2</sub> catalysts. (a) Polarization curves of S-MoS<sub>2</sub>, 1.1-V MoS<sub>2</sub>, Li-MoS<sub>2</sub>, and Pt wire. 1.1-V MoS<sub>2</sub> shows an improved HER activity than that of S-MoS<sub>2</sub> due to the formation of 1T phase MoS<sub>2</sub> and increased surface area. The performance of Li-MoS<sub>2</sub> is further enhanced as the percentage of 1T phase is increased from 1.1-V MoS<sub>2</sub>. (b) Tafel plots of S-MoS<sub>2</sub>, 1.1-V MoS<sub>2</sub>, Li-MoS<sub>2</sub>, and Pt wire.



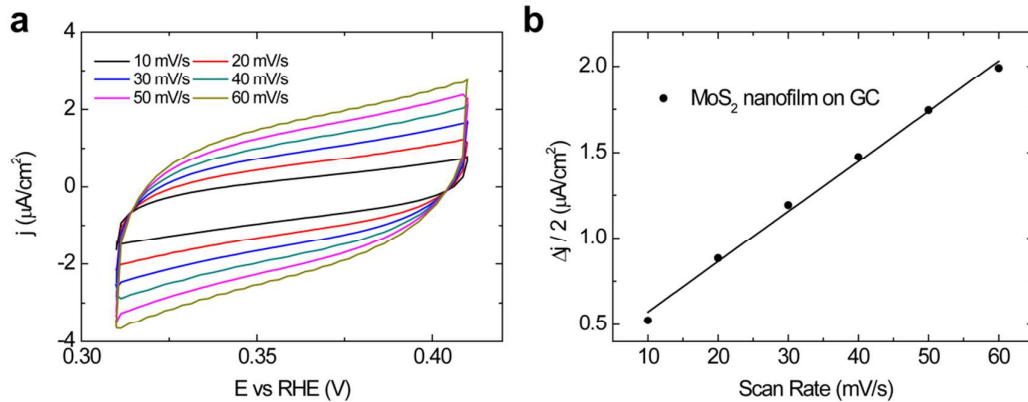


**Figure S8.** Electrochemical double layer capacitance measurement of MoS<sub>2</sub> nanofilm on flat glassy carbon substrate. (a) Electrochemical cyclic voltammogram of MoS<sub>2</sub> nanofilm at different potential scanning rates. The scan rates are 10, 20, 30, 40, 50, 60 mV/s respectively, due to the much smaller surface area compared with Li-MoS<sub>2</sub>. The selected potential range where no faradic current was observed is 0.31 to 0.41 V vs. RHE. (b) Linear fitting of the capacitive currents of the catalysts vs. scan rates. The calculated double layer capacitance is 29 μF/cm<sup>2</sup>. From Ref. 8 we know that the density of HER active sites in MoS<sub>2</sub> nanofilm is  $5.37 \times 10^{14}$  sites/cm<sup>2</sup>. Therefore, the density of the active sites in Li-MoS<sub>2</sub> sample is  $5.37 \times 10^{14}$  sites/cm<sup>2</sup>  $\times$  345000 / 29 =  $6.4 \times 10^{18}$  sites/cm<sup>2</sup>. At 200 mV overpotential we get 200 mA/cm<sup>2</sup> cathodic current, by which the TOF is calculated as follows:

$$\text{TOF (at 200 mV)} = \frac{0.2 \text{ A/cm}^2}{1.6 \times 10^{-19} \text{ C/e}^- \times 2 \text{ e}^-/\text{H}_2 \times 6.4 \times 10^{18} \text{ sites/cm}^2} = 0.1 \text{ H}_2/\text{s per site}.$$

Catalyst	Mass Loading	Tafel Slope	j @ - 200 mV vs RHE
Li-MoS <sub>2</sub> (current work)	~ 3.4 mg/cm <sup>2</sup>	62 mV/decade	200 mA/cm <sup>2</sup>
1T MoS <sub>2</sub> nanosheets <sup>36</sup>	0.05 mg/cm <sup>2</sup>	40 mV/decade	7 mA/cm <sup>2</sup>
Exfoliated 1T MoS <sub>2</sub> <sup>28</sup>	N/A	43 mV/decade	21 mA/cm <sup>2</sup>
MoS <sub>2</sub> NPs on graphene <sup>17</sup>	1 mg/cm <sup>2</sup>	41 mV/decade	43 mA/cm <sup>2</sup>
Double-gyroid MoS <sub>2</sub> <sup>26</sup>	0.06 mg/cm <sup>2</sup>	50 mV/decade	4 mA/cm <sup>2</sup>
Amorphous MoS <sub>2</sub> <sup>22</sup>	N/A	40 mV/decade	15 mA/cm <sup>2</sup>
MoS <sub>2</sub> sponges <sup>27</sup>	N/A	185 mV/decade	71 mA/cm <sup>2</sup>

**Table S1.** The mass loadings, Tafel slopes, and the cathodic currents at 200 mV overpotential of different MoS<sub>2</sub> catalysts.